CRYSTALLINE PROPERTIES OF MELT-PROCESSED POLYAMIDE 6 MATRIX MULTISCALE HYBRID COMPOSITES

József Szakács[1]; Roland Petrény[1]; László Mészáros[1,2]

[1] Department of Polymer Engineering, Faculty of Mechanical Engineering, Budapest University of Technology and Economics, Muegyetem rkp. 3. T bld. III., H-1111 Budapest, Hungary
[2] MTA–BME Research Group for Composite Science and Technology, Muegyetem rkp. 3., H-1111 Budapest, Hungary
corresponding author: László Mészáros, e-mail: meszaros@pt.bme.hu,
Phone: +36-1-463-1525
Fax: +36-1-463-1527

Abstract

We investigated the crystalline properties of injection molded polyamide 6 matrix composites containing carbon nanotubes and microfibers (basalt and carbon). We showed with differential scanning calorimetry (DSC) tests that microfibers affect crystalline properties differently. Basalt fibers do not have a nucleating effect, while carbon fibers do, to a small extent. Carbon nanotubes acted as nucleating agents themselves but in composites reinforced with microfibers they increased the crystallinity even more. Due to the nucleating effect of the nanotubes, crystallization started at a higher temperature in each composite. We observed synergistic effects concerning nucleation in hybrid composites. We decomposed the crystalline melting curves to determine the characteristics of the crystallite types and proved that the presence of nanotubes facilitated the formation of α-type crystallites. We showed that nanotubes have a double effect: they have a nucleating effect regarding crystallinity, and they inhibit the movement of polyamide molecules relative to each other, which decreases the tendency to crystallize. Therefore, nanotube content has an optimum concerning crystallization. This is in accordance with tensile mechanic properties.

Keywords: polyamide, carbon nanotube, fibers, crystallinity, polymorphism, DSC

Introduction

Modern technology heavily depends on polymers and polymer matrix composites. More and more fiber-reinforced polymer composites are used in engineering applications each year. As in other areas, miniaturization is gaining ground in the development of composites as well: the use of nanoparticles as reinforcement of polymer composites is one of the most researched areas [1-4].

Nanoparticles have come to the forefront because they have an exceptionally high specific surface area, therefore they show higher fill fraction in composites than other, conventional reinforcing materials. If they are uniformly dispersed, the interface between the nanoparticles and the matrix is so large that the weak interactions on the interface can considerably affect the properties of the composite [5, 6]. Of nanosized reinforcements, various carbon-based nanoparticles, especially carbon nanotubes, are especially important; they are among the highest strength materials that can be manufactured [7-10].

The greatest challenge in the case of nanocomposites is how to disperse them uniformly. For the sake of better matrix-reinforcement connection and more even dispersion, often functional groups are grafted on nanoparticles, but this chemical procedure results in defects in the structure of the particle and it can impair various properties. Another problem is that functionalization typically involves the use of strong acids and alkalis – this makes the use of such materials difficult on an industrial scale [11-15]. A novel method to evenly disperse nanotubes, even in an industrial environment, may be the use of nanotubes in thermoplastic hybrid composites which also have fiber reinforcement, because the high shear in the matrix during processing can break up the aggregates [16].

Such hybrid composites can only be processed with high-productivity industrial technologies effectively if fiber reinforcement consists of short fibers. Short carbon fibers are extremely popular reinforcements of injection molded polymer composites, due to their high

tensile strength and modulus, but basalt fibers are also gaining in popularity, owing to their lower price and good mechanical properties [17, 18]. In short fiber-reinforced hybrid composites, microfibers are responsible for high strength and modulus, and the uniform dispersion of nanotubes, while nanoparticles change the functional properties of the matrix material (conductivity, flame retardancy etc.), but they can also effectively change strength and affect the crystallization properties of the matrix. This latter area has been little researched so far, at least in hybrid composites [19, 20].

Hybrid composites containing fiber reinforcement can only be manufactured with high productivity, industrial technologies if the matrix is thermoplastic. Various polyamides are popular matrix materials of high-performance composites, due to their excellent mechanical properties. These outstanding mechanical properties are partly the result of their semicrystalline structure [21]. Carbon nanotubes in nanocomposites can affect the crystalline structure of the polyamide, as nanoparticles often act as nucleating agents in semicrystalline polymers. This is because in polymers, a general way of the forming of nuclei is heterogeneous nucleation, that is, crystallization is started by an inhomogeneity in the melt. In nanocomposites, the inhomogeneities are the nanoparticles, which can therefore initiate crystallization [22, 23]. This means that, for example, with carbon nanotubes, a higher crystalline fraction can be achieved and the structure is finer as the average size of crystallites is smaller. Both phenomena affect mechanical properties, for example, as crystallinity grows, strength also grows [24, 25]. Nanotubes are inside the crystallites (as they are heterogeneous nucleating agents); therefore they have a strong connection with the crystallite and can effectively affect properties [7, 26, 11, 27-29]. It, however, always depends on the system whether a given nanoparticle in a given matrix increases or decreases crystallinity. [30-32]. Zhou et al [33] observed that in PA 6 matrix, carbon nanotube-reinforced composites, an increase in nanotube content caused an increase in crystallinity, and a second crystallization peak appeared on the DSC curve, which shifted to

3

higher temperatures as nanotube content increased. This suggests that evenly distributed CNT in the PA6 matrix acted as a heterogeneous nucleating agent. The degree of the nucleating effect of carbon nanotubes largely depends on how uniformly nanotubes are dispersed in the matrix—if the nanotubes form aggregates, they may even inhibit crystallization [34]. In fiber-reinforced composites, short fibers can also act as nucleating agents, similarly to nanoparticles, but at a high volume fraction they can hinder crystallization [35, 36]. Therefore, in hybrid composites, both carbon nanotubes and carbon or basalt fibers can be initiators of crystallization, and by increasing the crystalline fraction, they can also improve the mechanical properties of the composite indirectly.

Well-distributed particles can not only serve as reinforcement in the matrix, but due to their size, they can also considerably change the morphology of the matrix around them; by increasing crystallinity, they can improve the mechanical properties of the matrix indirectly. As mentioned before, carbon nanotubes and various short fibers can act as nucleating agents and can increase the thermal conductivity of the composite, which facilitates overcooling. It promotes crystallization and can result in more homogeneous temperature distribution during cooling. Faster cooling, however, impairs crystal growth, which can decrease crystallinity [37].

The crystallites in polyamide 6 can be α-type and γ-type stable crystallites. In the α-type crystallite structure, the molecular chains of the polyamide 6 are stretched, are in anti-parallel relative positions and form a monoclinic crystal structure consisting of plates, while in the γ-type structure, the chains are twisted, are in parallel relative positions, and as a result, the angle of the H-bonds between the chains changes to approximately 60°. In the α-type crystallites, the stretched polyamide chains are not only more stable thermodynamically but also have higher tensile strength and modulus. The greater stability of the α-type structure is also represented in its higher crystalline melting temperature of ~223°C, while in the case of the γ-type structure, it is ~215°C. Crystallization at a higher temperature (above 190°C) results in the formation of

the α-type crystallite structure, while the γ-type crystal typically forms at lower temperatures (under 140°C); between these two temperatures, both crystallite types can be expected in different amounts. Carbon nanotubes cause crystallization to start at a higher temperature. This promotes the formation of α crystals, which results in better strength properties [19, 20, 38].

We published the effect of the individual components of polyamide 6 matrix hybrid composites reinforced with carbon fibers or basalt fibers on mechanical properties, and a detailed analysis of the mechanical properties (at different loads) in an earlier article of ours [39]. Reinforcements, however, do not only change mechanical properties through their reinforcing effect but also through their effect on the morphology. The goal of this research is to reveal the effect of fibers and nanotubes on the crystalline fraction of the PA6 matrix and the properties of the crystallite structure and their effect on mechanical properties in injection molded hybrid composites containing CNT and basalt or carbon fibers.

Experimental

Materials

Schulamid 6 MV 13 type polyamide 6 (PA 6) from A. Schulman GmbH (Germany) was used as matrix material. BCS KV02 type basalt fiber (BF) from Kamenny Vek Ltd. (Russia) and Panex 35 type 95 carbon fiber (CF) from Zoltek Zrt (Hungary) was applied as micro-sized reinforcement. The initial length of both fibers was 6 mm. The average diameter of basalt fibers was 15.6±1.9 μm and that of the carbon fibers was 8.3±1.0 μm. NANOCYL NC7000 carbon nanotubes supplied by Nanocyl SA. (Belgium) were used as nanosize reinforcement. Nanotubes had an average length of 1.5 μm and their average diameter was 9.5 nm. The minimal carbon purity of nanotubes was 90% and nanotubes had no surface treatment.

Sample Preparation

A Labtech Scientific type twin-screw extruder (L/D=44; D=26 mm) was used for continuous melt mixing. Screw speed was 25 min^{-1} and extrusion temperature was 250 °C.

30 mass% BF or CF and 0.25, 0.5, 0.75, or 1 mass% CNT was used for the different composites (Table 1.). Dried PA 6 granules (80 °C; 4 hours) were mechanically mixed with the reinforcing materials for two minutes. After that, every 5 minutes, they were remixed for 10 seconds to avoid settling, then extruded and granulated (particle size: 4.5 mm). Dumbbell-shaped specimens (type 1A according to the ISO 527-2 standard) were injection molded on an Arburg Allrounder Advance 370S 700-290 injection molding machine. Injection molding temperature was 275 °C and maximal pressure was 800 bar. Mold temperature was set to 80°C.

Tensile tests

Before the mechanical tests, the specimens were conditioned at 50% relative humidity at room temperature for a month, then the temperature was set to 25°C (relative humidity remained 50%) for a further week. Tensile tests were performed on a Zwick Z020 (Germany) universal testing machine according to EN ISO 527. The crosshead speed was 5 mm min^{-1} during tensile tests and 5 specimens were tested from each material type.

Scanning electron microscopy

The fracture surfaces of the broken tensile tested specimens were investigated with a Jeol 6380 LA type scanning electron microscope (SEM) after they were sputtered with a thin gold layer.

Differential Scanning Calorimetry (DSC)

The crystallization peaks and crystalline fraction of PA6 and PA6 composites were determined with a TA Instruments Q2000 Differential Scanning Calorimeter. The heating and cooling rate was 10 °C min^{-1}. The tests were performed in an inert atmosphere (N$_2$; 50 ml min^{-1}-flow rate). Polyamide 6 has two stable (α and γ) crystalline types, which have different melting temperatures and melting heats. For this reason, when the crystalline fraction is determined, an

average melting heat can be used, which in our case was 240 Jg^{-1} [20]. The crystalline fraction was calculated with Eq. 1.

$$X_k = \frac{X_m}{X_a \cdot (1-\varphi)},$$ (1)

where X_m is the measured crystalline melting heat, X_a is the average crystalline melting heat of the 100% crystalline polyamide, and φ is the fiber content in mass%. In an injection molded polymer product, the crystalline properties can be different along the thickness of the product, due to the core-shell structure, therefore, for the sake of comparability, we made the samples from the central part of the specimen, which was in the center of the flow path.

Results and discussion

Tensile properties

The tensile tests showed that if there are only nanoparticles in the system, both strength and tensile elasticity and decrease, while elongation at break changes only very little (Table 2.). In other words, nanoparticles do not have a strengthening effect. This is because a large proportion of nanoparticles did not disperse in the matrix but formed aggregates. The fracture surface of the tensile specimen shows such an aggregate and its environment clearly (Fig. 1a). It can be seen that on the one hand, the aggregate was the starting point of the fracture and also that the aggregate has two parts. Its outer part is soaked with the matrix, while inside there are only nanotubes. In the matrix we found some separate nanotubes but this was not characteristic. Decreasing strength is due to the fact that the aggregates act as stress concentration points, while reduced modulus is due to the fact that the part of the aggregates with no matrix do not have a load-bearing function, therefore the load-bearing cross section is decreased, which results in lower modulus. When there were also microparticles in the system, the nanoparticles also performed a reinforcing function. In the case of both carbon fiber and basalt fiber reinforcement,

nanoparticles were dispersed in the matrix well (Fig. 1b, c). Typically, up to 0.5 mass% nanotube content, strength and modulus increased; over that they started to decrease. We did not find aggregates on the fracture surfaces, which indicates that failure was due to fiber breaking or loss of microfiber-matrix adhesion. Since fiber-matrix adhesion did not change chemically, the strength reduction over 0.5 mass% in hybrid composites is definitely due to the changed behavior of the matrix. Increasing nanotube content makes the matrix more and more rigid and so the matrix can transmit the load less and less. This is because the molecular chains of the polymer connect to the nanotubes, therefore they lose some of their mobility, and plastic deformation is less characteristic to the system. Therefore, although chemical compatibility between the matrix and the reinforcing fibers continues to be adequate, as the mechanical properties of the matrix change, mechanical compatibility is impaired. The inhibited movement of the molecules also affects the crystallization of the matrix.

Investigation of the crystalline properties of the composites

The first heating curves of hybrid composites containing basalt or carbon fibers are similar to those of the pure matrix or nanocomposites (Fig. 2a-c). The crystalline fractures at the first heating indicate that the presence of nanotubes increased crystalline fracture (Fig. 2d). In the case of composites containing only nanotubes crystallinity grows moderately, but a minor decrease can be observed at the highest CNT content. This can be explained with the fact that higher CNT content may hamper the mobility of polyamide chains, which influences the crystallization process. This molecule localization effect can be attributed to two causes: on the one hand, the nanotubes, due to their high surface-to-weight ratio, connect to the polymer molecule in many places, and on the other hand, the size of the nanotubes is comparable to the size of the polymer molecules, therefore the polymer molecules can get entangled with them, which also inhibits the motion of the molecules. Also, the effect of nanotubes used alone is far weaker than if used together with, e.g. basalt fibers in hybrid composites. This can be explained

8

with the presence of aggregates presented in the Tensile properties section. If nanotubes are less dispersed, their effect is weaker. Also, in hybrid composites, thanks to better dispersion, the above-mentioned localizing effect is also stronger, as a result of which, the maximum of crystallinity is at 0.25 mass% nanotube content.

The curves registered during cooling indicate that the presence of microfibers did not particularly affect crystallization. On the other hand, the presence of CNT helps start crystallization: with CNT, crystallization starts at a higher temperature, that is, CNT acts as a nucleating agent (Fig. 3a-c). The process of crystallization is very similar to what Phang et al [40] described. They showed that in the presence of nanotubes, a shoulder appears at a higher temperature than the original, which indicates a second crystallization peak. Moreover, this peak shifts to higher temperatures as nanotube content is increased. Brosse et al [31] showed that the appearance of the second crystallization peak indicates the crystallization of the trans-crystalline lamellae from the surface of nanotubes through epitaxial growth. They also showed that the size of this peak is directly related to the dispersion of the nanotubes. In the case of our hybrid composites, there is also a peak at a higher temperature, which is bigger than in the curves of composites containing only nanotubes—as nanotube content increases, the shoulder becomes more pronounced. Table 3. shows the Crystalline melting- and crystallization temperatures registered with DSC. The DSC curves of both nanocomposites and hybrid composites show that the crystalline melting temperature (in the case of both the first and the second heating; T_{m1}; T_{m2}) is shifted very slightly towards lower temperatures (differences are mostly within standard deviation). For all practical purposes, the values can be considered unchanged. The explanation may be that nanotubes and basalt or carbon fibers improve the thermal conductivity of the composite, and therefore help crystal melting during measurement. Analyzing the peak temperatures of the cooling curves (T_c) gives a clearer picture of the effect of the different components on crystallization. On the one hand, BF did not change the value,

that is, did not affect crystallization very much. This corresponds to what we experienced during the first heating, since the crystalline fraction there did not change compared to the pure matrix. In the presence of carbon fibers, the temperature of the crystallization peak is a little bit higher, which can also be attributed to the increased crystalline fraction experienced at the first heating. The presence of nanotubes resulted in an increase of the crystallization peak temperature but his effect seems independent of the amount of nanotubes. In other words, in the case of the examined nanotube contents, the presence of nanotubes is important, not their dispersion.

During the first heating, the thermal history of the material caused by the manufacturing technology can be examined, while during the second heating, the properties of the material, which are independent of the technology, can be analyzed. As opposed to the first heating, two easily noticeable peaks can be observed on the melting curve of the polyamide (Fig. 4a): at 216.5°C and at 220.5°C. These temperatures are the melting peaks of the γ-type (lower) and the α-type (higher) crystallites. This is because the melt cools and solidifies much faster during injection molding than during a DSC test, and in the latter case, there is enough time for the γ-type crystals to form. [41, 42].

On the curves of composites containing only nanotubes, the conspicuous first peak disappears, which indicates that the ratio of γ-type crystallites decreased considerably, while the ratio of more stable α crystallites grew, and crystallinity also increased. Basalt fiber reinforced and carbon fiber reinforced composites behave similarly (Fig. 4/b-c): on the DSC curves of composites reinforced only with fibers; similarly to the matrix, a relatively large γ crystalline peak can be observed, while the curves of composites also containing nanotubes do not have this peak, and the crystalline fraction increases.

The melting curves can be decomposed into two parts and this way the ratio of the crystallite types can be estimated better. A common practice is to approximate DSC curves with a Gauss curve, but it only approximates the melting curve, as the curve is not symmetrical due

to the different crystallite sizes. For this reason, this approximation would show more γ-type crystallites. Therefore, instead of the Gauss curve, we used the asymmetric double sigmoid curve, which can approximate the melting curve more accurately. This sigmoid curve has so far mostly been used in food industry tests [43, 44]. The function can be written in the following form Eq. 2.:

$$y = y_0 + A \frac{1}{1+e^{-\frac{x-x_c+w_1/2}{w_2}}} \left(1 - \frac{1}{1+e^{-\frac{x-x_c-w_1/2}{w_3}}}\right)$$
(2)

The function has six parameters; y_0 is shift, x_c is its average (expected value), A is amplitude, w_1 is the full width of the curve at half maximum, w_2 is the variance of the lower side, w_3 is the variance of the upper side. The result of fitting the function can be seen in Fig. 6/a. The sigmoid function can produce good fitting ($R^2>0.998$), and the ratios of the crystallite types can also be analyzed. The crystal melting enthalpy is necessary for the calculation of the ratio of the crystallites. For α- and γ-type crystallites, the same melting enthalpy was taken in this study, which was 240 Jg^{-1} [20].

The decomposition of the curves (Fig. 5a) show that adding a small amount of carbon nanotubes resulted in an 8% increase in the ratio of α-type crystallites (Fig. *5b*).

It started to decrease again at higher CNT contents, but even at 1 mass% CNT content, it was still higher than in the case of pure polyamide. When CNT content is low, crystallization starting at higher temperatures results in a larger amount of more stable α-type crystallites, but too much CNT can hamper crystallization because when the large aggregates swell, the mobility of some of the chains decreases considerably. Decreased mobility leads to slower ordering and this favors the formation of γ-type crystallites.

In the basalt fiber reinforced composite (Fig. 5b.), the ratio of α-type crystallites is lower than in the neat polyamide, but an addition of only 0.25 mass% CNT raised it over that of the neat polyamide, and even more CNT increased the ratio of α crystals even further. In carbon

fiber reinforced composites, the ratio of α-type crystallites increased compared to neat polyamide, and the addition of CNT increased the ratio even higher, that is, here both carbon fibers and carbon nanotubes acted as α nucleating agents. In composites containing only carbon nanotubes, the ratio of α crystallites starts to decrease at a CNT content of only 0.5 mass% CNT, while in fiber-reinforced hybrid composites reduction only starts at 1 mass% nanotube content, which also indicates that fibers facilitate the uniform dispersion of nanotubes, which can act as α nucleating agents far more effectively. The general conclusion is that regardless of reinforcing materials, in a polyamide 6 matrix, carbon nanotubes promote the formation of the more stable α crystals, because they start crystallization at a higher temperature. A higher temperature favors the formation of α-type crystallites because of the higher mobility of chains; the ratio of γ-type crystallites decreases.

Summary

We investigated the crystalline structure of novel hybrid composites, which can be manufactured in an industrial environment. The crystallinity of composites containing only nanotubes increased as nanotube content increased, with the highest value reached at 0.5 mass% CNT. The crystallinity of hybrid composites also containing basalt or carbon fibers reached even higher values. The explanation of this synergistic effect is that the microfibers facilitated the more uniform dispersion of nanotubes, thus promoting their nucleating effect. Nanotubes also affected the structure of crystallites; as heterogeneous nucleating agents, they promoted crystallization starting at a higher temperature, and epitaxial crystal growth was also exhibited. Overall, this nucleating effect resulted in the formation of the more stable α-type crystallites. α crystallites have higher strength and modulus than γ crystallites; therefore carbon nanotubes can also improve the strength and modulus of composites indirectly, by changing the crystalline structure. Increased nanotube content increased the ratio of α-type crystallites. The effect of

nanotubes first increases as their amount increases, then above a certain amount, it starts decreasing. This is because nanotubes, due to their high surface-to-weight ratio, connect to the molecules of the matrix in many places (even in the melt state), and the molecules are entangled with the nanotubes. This all inhibits the movement of the molecules, therefore above a certain nanotube content, they do not increase crystallinity. This can all be related to mechanical properties and the degree of dispersion.

Acknowledgements

References

1. Gumede TP, Luyt AS, Muller AJ. Review on PCL, PBS, and PCL/PBS blends containing carbon nanotubes. Express Polym Lett. 2018;12:505-29. doi:https://doi.org/10.3144/expresspolymlett.2018.43.

2. Wang FX, Liang WY, Wang ZQ, Yang B, He L, Zhang K. Preparation and property investigation of multi-walled carbon nanotube (MWCNT)/epoxy composite films as high-performance electric heating (resistive heating) element. Express Polym Lett. 2018;12:285-95. doi:https://doi.org/10.3144/expresspolymlett.2018.26.

3. Tahouneh V. An elasticity solution for vibration analysis of laminated plates with functionally graded core reinforced by multi-walled carbon nanotubes. Period Polytech Mech. 2017;61(4):309-19. doi:https://doi.org/10.3311/PPme.11254.

4. Jalalvand M, Czél G, Wisnom MR. Damage analysis of pseudo-ductile thin-ply UD hybrid composites – A new analytical method. Compos Part A-Appl S. 2015;69:83-93. doi:https://doi.org/10.1016/j.compositesa.2014.11.006.

5. Rafiq R, Cai D, Jin J, Song M. Increasing the toughness of nylon 12 by the incorporation of functionalized graphene. Carbon. 2010;48(15):4309-14. doi:https://doi.org/10.1016/j.carbon.2010.07.043.

6. Chen G-X, Kim H-S, Park BH, Yoon J-S. Multi-walled carbon nanotubes reinforced nylon 6 composites. Polymer. 2006;47(13):4760-7. doi:https://doi.org/10.1016/j.polymer.2006.04.020.

7. Friedrich K, Fakirov S, Zhang Z. Polymer Composites: From Nano-to-macro-scale. Springer; 2005.

8. Lee C, Wei X, Kysar JW, Hone J. Measurement of the elastic properties and intrinsic strength of monolayer graphene. Science. 2008;321(5887):385-8. doi:https://doi.org/10.1126/science.1157996.

9. Yu M-F, Lourie O, Dyer MJ, Moloni K, Kelly TF, Ruoff RS. Strength and breaking mechanism of multiwalled carbon nanotubes under tensile load. Science. 2000;287(5453):637-40. doi:10.1126/science.287.5453.637.

10. Ruoff RS, Qian D, Liu WK. Mechanical properties of carbon nanotubes: theoretical predictions and experimental measurements. C R Phys. 2003;4(9):993-1008. doi:https://doi.org/10.1016/j.crhy.2003.08.001.

11. Ma P-C, Siddiqui NA, Marom G, Kim J-K. Dispersion and functionalization of carbon nanotubes for polymer-based nanocomposites: A review. Compos Part A-Appl S. 2010;41(10):1345-67. doi:https://doi.org/10.1016/j.compositesa.2010.07.003.

12. Rahmat M, Hubert P. Carbon nanotube–polymer interactions in nanocomposites: A review. Compos Sci Technol. 2011;72(1):72-84. doi:https://doi.org/10.1016/j.compscitech.2011.10.002.

13. Sahoo NG, Cheng HKF, Cai J, Li L, Chan SH, Zhao J et al. Improvement of mechanical and thermal properties of carbon nanotube composites through nanotube functionalization and processing methods. Mater Chem Phys. 2009;117(1):313-20. doi:https://doi.org/10.1016/j.matchemphys.2009.06.007.

14. Scaffaro R, Maio A, Tito AC. High performance PA6/CNTs nanohybrid fibers prepared in the melt. Compos Sci Technol. 2012;72(15):1918–23. doi:10.1016/j.compscitech.2012.08.010.

15. Wei C, Cho K, editors. Chemical Bonding of Polymer on Carbon Nanotube. Mater Res Soc Symp P; 2001. San Francisco

16. Karsli GN, Yesil S, Aytac A. Effect of hybrid carbon nanotube/short glass fiber reinforcement on the properties of polypropylene composites. Compos Part B-Eng. 2014;63:154-60. doi:https://doi.org/10.1016/j.compositesb.2014.04.006.

17. Fiore V, Scalici T, Di Bella G, Valenza A. A review on basalt fibre and its composites. Compos Part B-Eng. 2015;74:74-94. doi:https://doi.org/10.1016/j.compositesb.2014.12.034.

18. Morgan P. Carbon fibers and their composites. Boca Raton: CRC Press; 2005.

19. Shen L, Tjiu WC, Liu T. Nanoindentation and morphological studies on injection-molded nylon-6 nanocomposites. Polymer. 2005;46(25):11969-77. doi:https://doi.org/10.1016/j.polymer.2005.10.006.

20. Fornes TD, Paul DR. Crystallization behavior of nylon 6 nanocomposites. Polymer. 2003;44(14):3945-61. doi:https://doi.org/10.1016/S0032-3861(03)00344-6.

21. Page IB. Polyamides as engineering thermoplastic materials. Shrewsbury: Rapra Technology Limited; 2000.

22. Strobl GR. The physics of polymers. Berlin: Springer-Verlag; 2007.

23. Piorkowska E, Rutledge GC. Handbook of polymer crystallization. Hoboken, New Jersey: John Wiley & Sons, Inc.; 2013.

24. Bessell TJ, Hull D, Shortall JB. The effect of polymerization conditions and crystallinity on the mechanical properties and fracture of spherulitic nylon 6. J Mater Sci. 1975;10(7):1127-36. doi:https://doi.org/10.1007/BF00541393.

25. El-Hadi A, Schnabel R, Straube E, Müller G, Henning S. Correlation between degree of crystallinity, morphology, glass temperature, mechanical properties and biodegradation of poly (3-hydroxyalkanoate) PHAs and their blends. Polym Test. 2002;21(6):665-74. doi:https://doi.org/10.1016/S0142-9418(01)00142-8.

26. Liu W-W, Chai S-P, Mohamed AR, Hashim U. Synthesis and characterization of graphene and carbon nanotubes: A review on the past and recent developments. J Ind Eng Chem. 2014;20(4):1171-85. doi:https://doi.org/10.1016/j.jiec.2013.08.028.
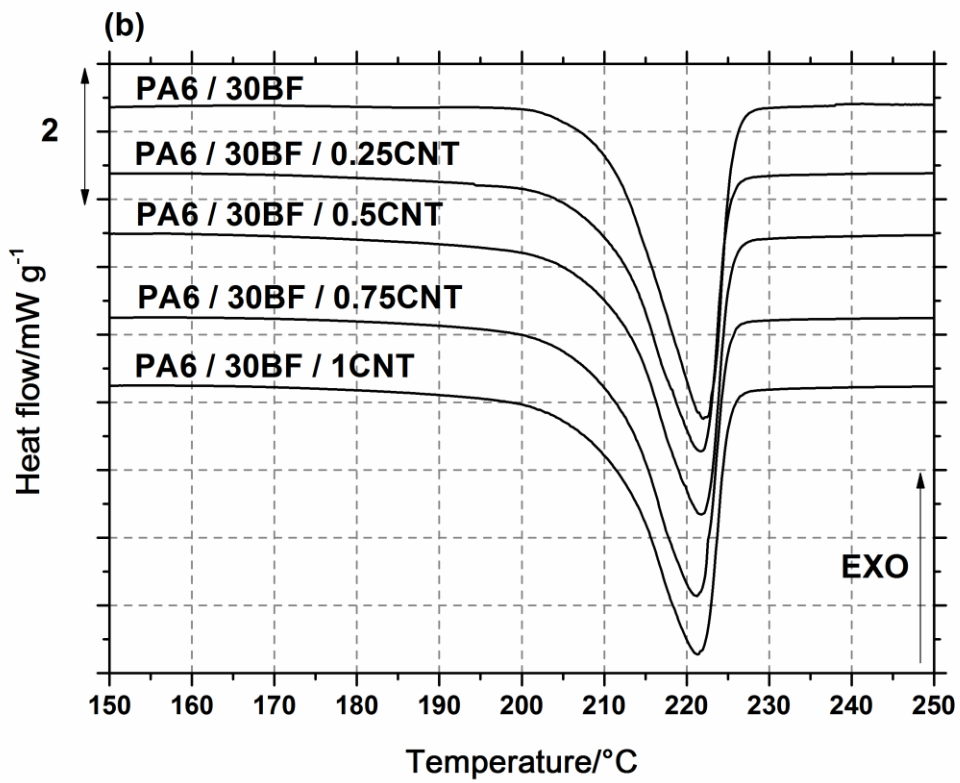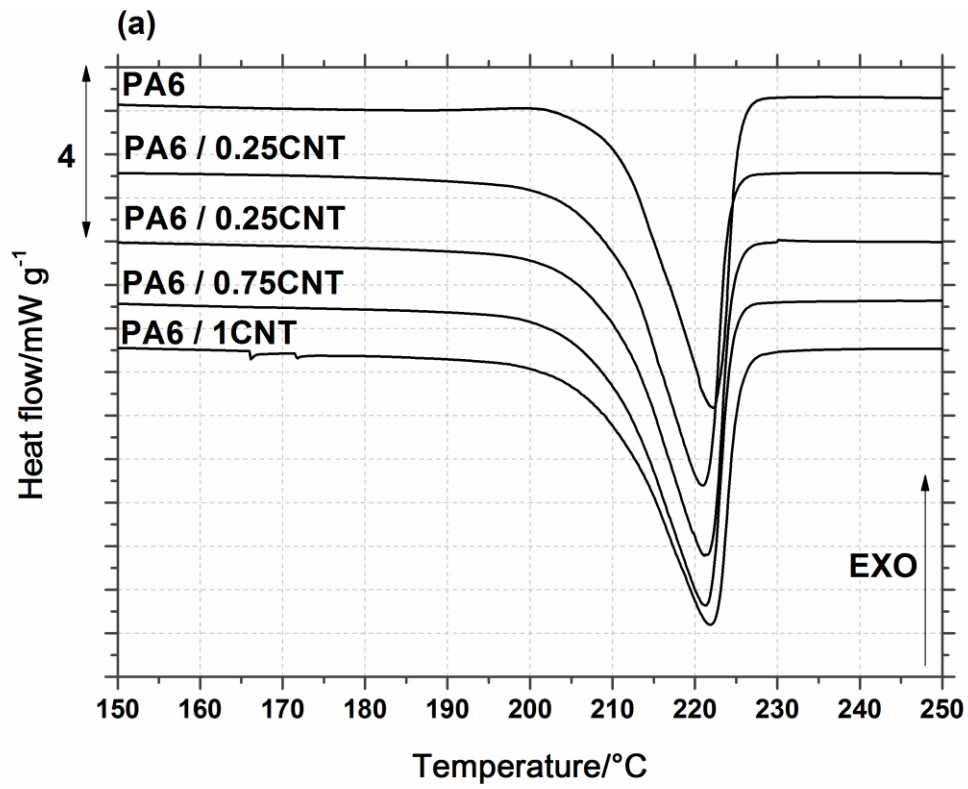
27. Jancar J, Douglas JF, Starr FW, Kumar SK, Cassagnau P, Lesser AJ et al. Current issues in research on structure–property relationships in polymer nanocomposites. Polymer. 2010;51(15):3321-43. doi:https://doi.org/10.1016/j.polymer.2010.04.074.

28. Singh V, Joung D, Zhai L, Das S, Khondaker SI, Seal S. Graphene based materials: Past, present and future. Prog Mater Sci. 2011;56(8):1178-271. doi:https://doi.org/10.1016/j.pmatsci.2011.03.003.

29. Meng H, Sui GX, Xie GY, Yang R. Friction and wear behavior of carbon nanotubes reinforced polyamide 6 composites under dry sliding and water lubricated condition. Compos Sci Technol. 2009;69(5):606-11. doi:https://doi.org/10.1016/j.compscitech.2008.12.004.

30. Chiu F-C, Huang IN. Phase morphology and enhanced thermal/mechanical properties of polyamide 46/graphene oxide nanocomposites. Polym Test. 2012;31(7):953-62. doi:https://doi.org/10.1016/j.polymertesting.2012.06.014.

31. Brosse A-C, Tencé-Girault S, Piccione PM, Leibler L. Effect of multi-walled carbon nanotubes on the lamellae morphology of polyamide-6. Polymer. 2008;49(21):4680-6. doi:https://doi.org/10.1016/j.polymer.2008.08.003.

32. Jin J, Rafiq R, Gill YQ, Song M. Preparation and characterization of high performance of graphene/nylon nanocomposites. Eur Polym J. 2013;49(9):2617-26. doi:https://doi.org/10.1016/j.eurpolymj.2013.06.004.

33. Zhou S, Hrymak AN, Kamal MR. Electrical, morphological and thermal properties of microinjection molded polyamide 6/multi-walled carbon nanotubes nanocomposites. Compos Part A-Appl S. 2017;103:84-95. doi:https://doi.org/10.1016/j.compositesa.2017.09.016.

34. Valentini L, Biagiotti J, López-Manchado MA, Santucci S, Kenny JM. Effects of carbon nanotubes on the crystallization behavior of polypropylene. Polym Eng Sci. 2004;44(2):303-11. doi:https://doi:10.1002/pen.20028.

35. Tan JK, Kitano T, Hatakeyama T. Crystallization of carbon fibre reinforced polypropylene. J Mater Sci. 1990;25(7):3380-4. doi:https://doi.org/10.1007/BF00587701.

36. Frihi D, Layachi A, Gherib S, Stoclet G, Masenelli-Varlot K, Satha H et al. Crystallization of glass-fiber-reinforced polyamide 66 composites: Influence of glass-fiber content and cooling rate. Compos Sci Technol. 2016;130:70-7. doi:https://doi.org/10.1016/j.compscitech.2016.05.007.

37. Schawe JEK. Cooling rate dependence of the crystallinity at nonisothermal crystallization of polymers: A phenomenological model. J Appl Polym Sci. 2016;133(6). doi:https://doi.org/doi:10.1002/app.42977.

38. Dasgupta S, Hammond WB, Goddard WA. Crystal structures and properties of nylon polymers from theory. J Am Chem Soc. 1996;118(49):12291-301. doi:https://doi.org/10.1021/ja944125d.

39. Szakács J, Mészáros L. Synergistic effects of carbon nanotubes on the mechanical properties of basalt and carbon fiber-reinforced polyamide 6 hybrid composites. J Thermoplast Compos. 2018;31(4):553-71. doi:10.1177/0892705717713055.

40. Phang IY, Ma J, Shen L, Liu T, Zhang W-D. Crystallization and melting behavior of multi-walled carbon nanotube-reinforced nylon-6 composites. Polym Int. 2006;55(1):71-9. doi:https://doi.org/doi:10.1002/pi.1920.

41. Wu B, Gong Y, Yang G. Non-isothermal crystallization of polyamide 6 matrix in all-polyamide composites: crystallization kinetic, melting behavior, and crystal morphology. J Mater Sci. 2011;46(15):5184-91. doi:https://doi.org/10.1007/s10853-011-5452-5.

42. Liang J, Xu Y, Wei Z, Song P, Chen G, Zhang W. Mechanical properties, crystallization and melting behaviors of carbon fiber-reinforced PA6 composites. J Therm Anal Calorim. 2014;115(1):209-18. doi:https://doi.org/10.1007/s10973-013-3184-2.
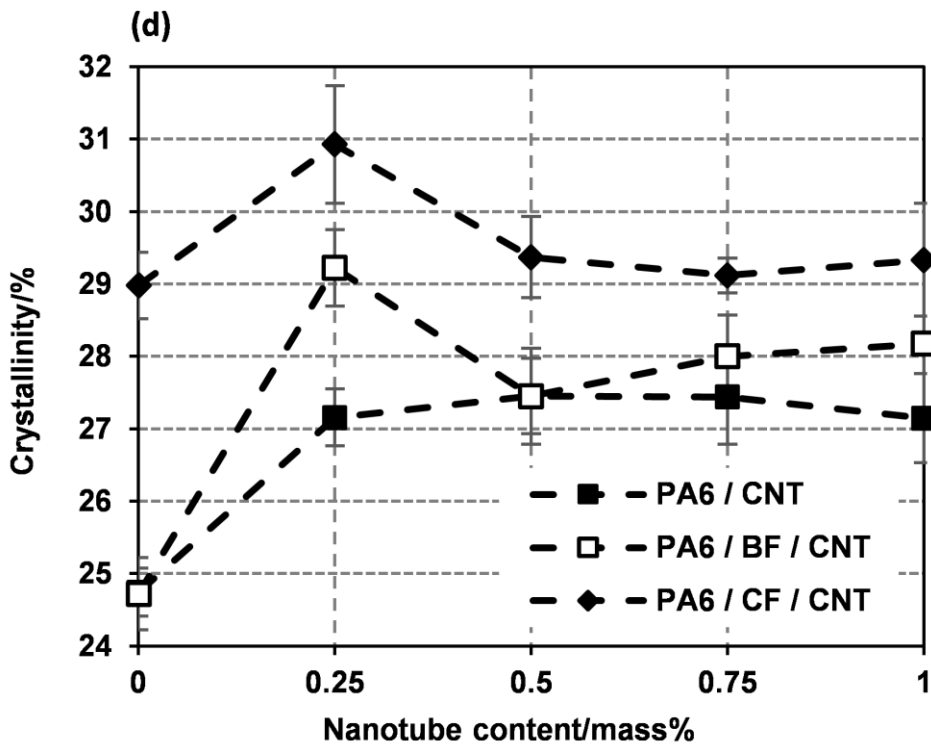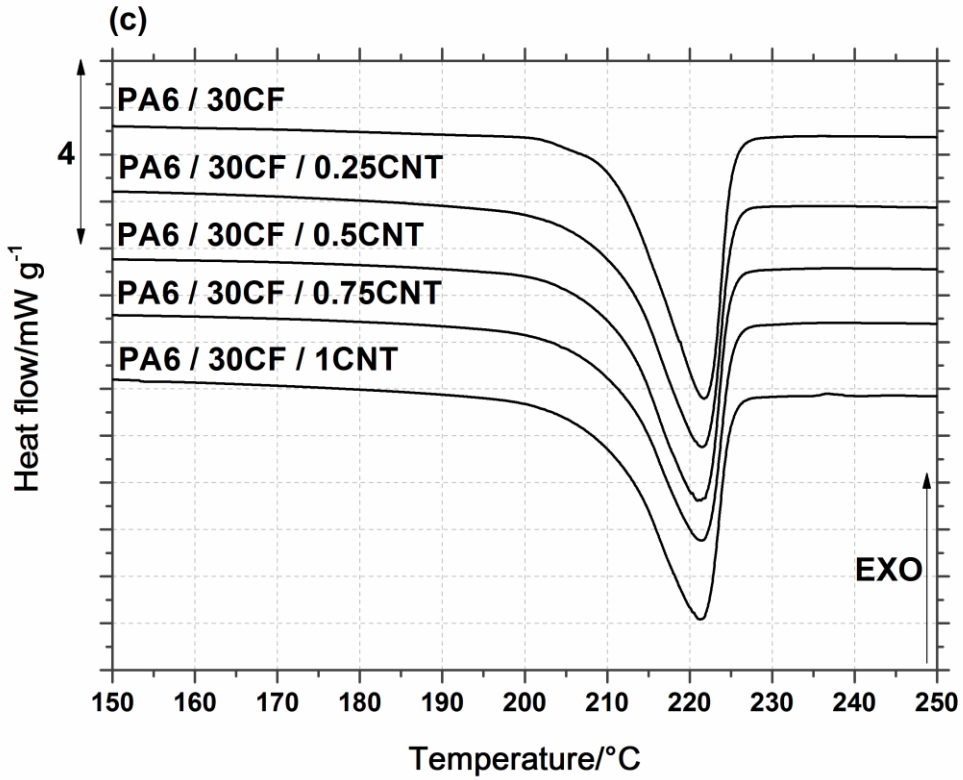
43. Vodovotz Y, Hallberg L, Chinachoti P. Effect of aging and drying on thermomechanical properties of white bread as characterized by dynamic mechanical analysis (DMA) and differential scanning calorimetry (DSC). Cereal Chem. 1996;73(2):264-70.

44. Höhne GWH, Hemminger W, Flammersheim HJ. Differential scanning calorimetry: An introduction for practitioners. 2 ed. Berlin: Springer-Verlag Berlin Heidelberg; 2003.
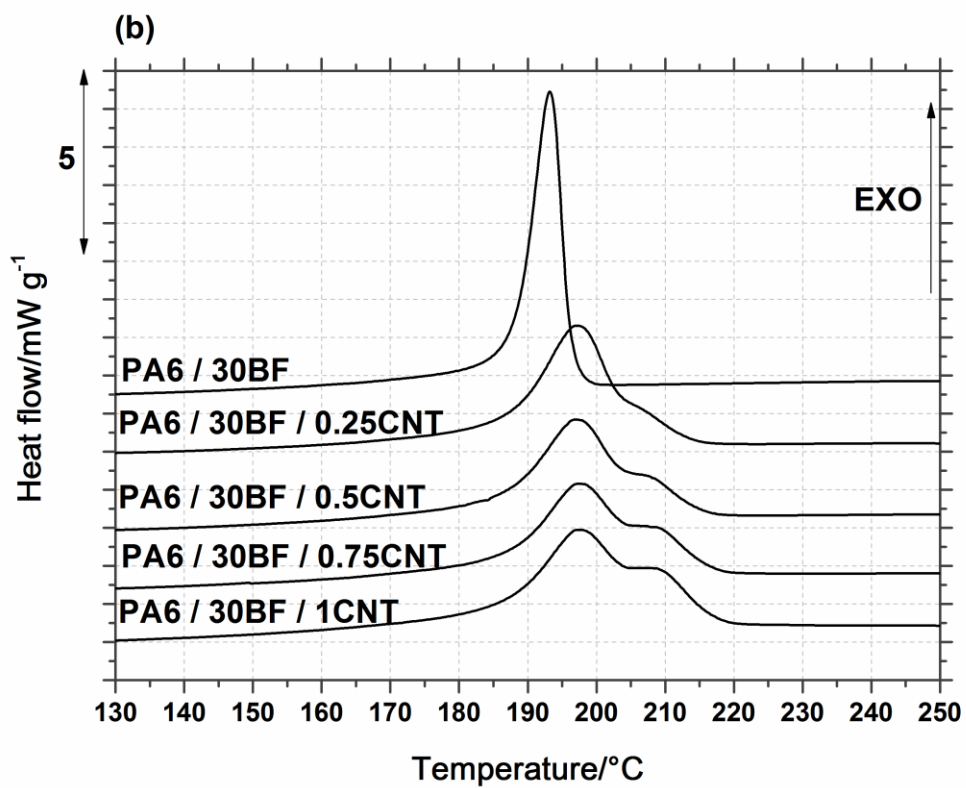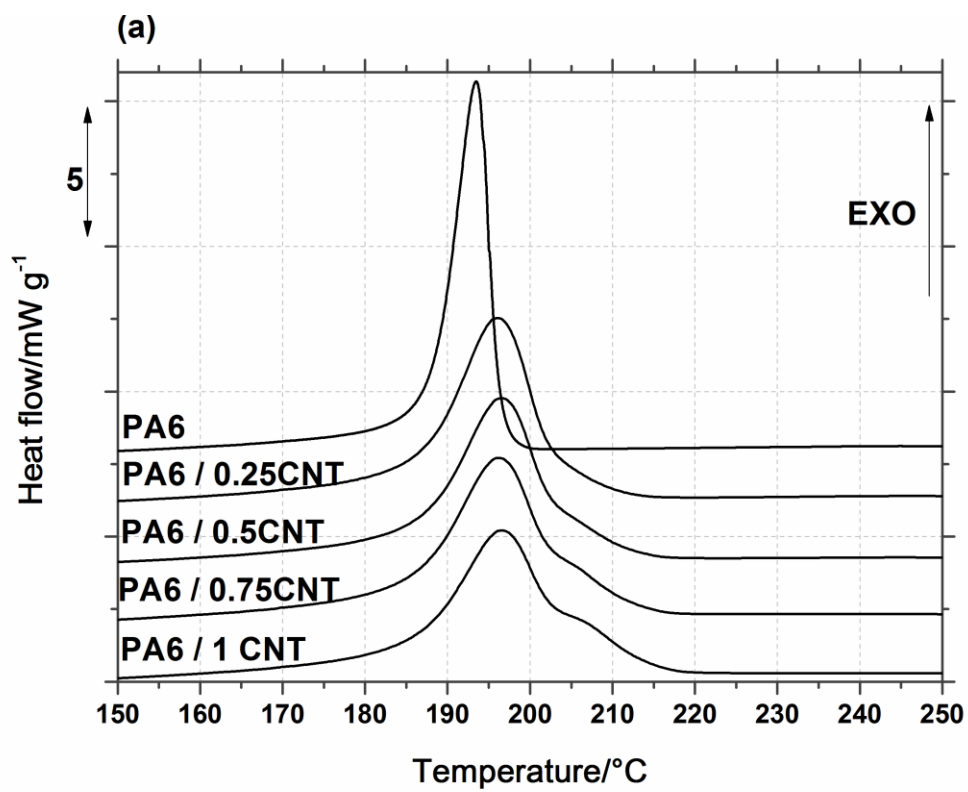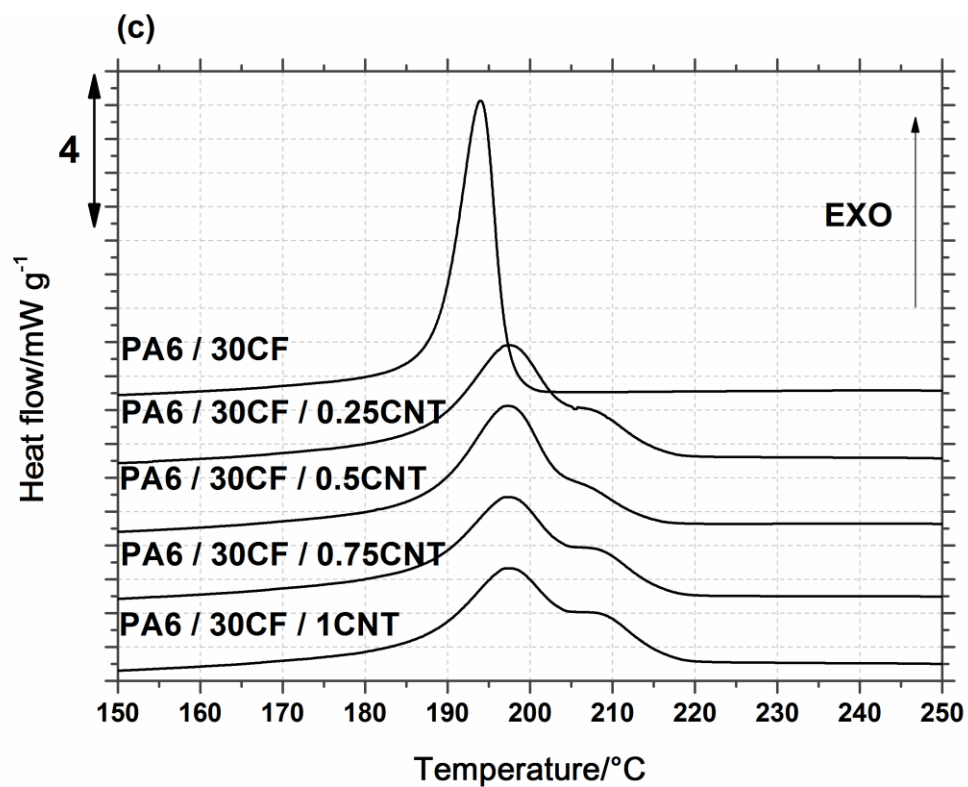
Figures
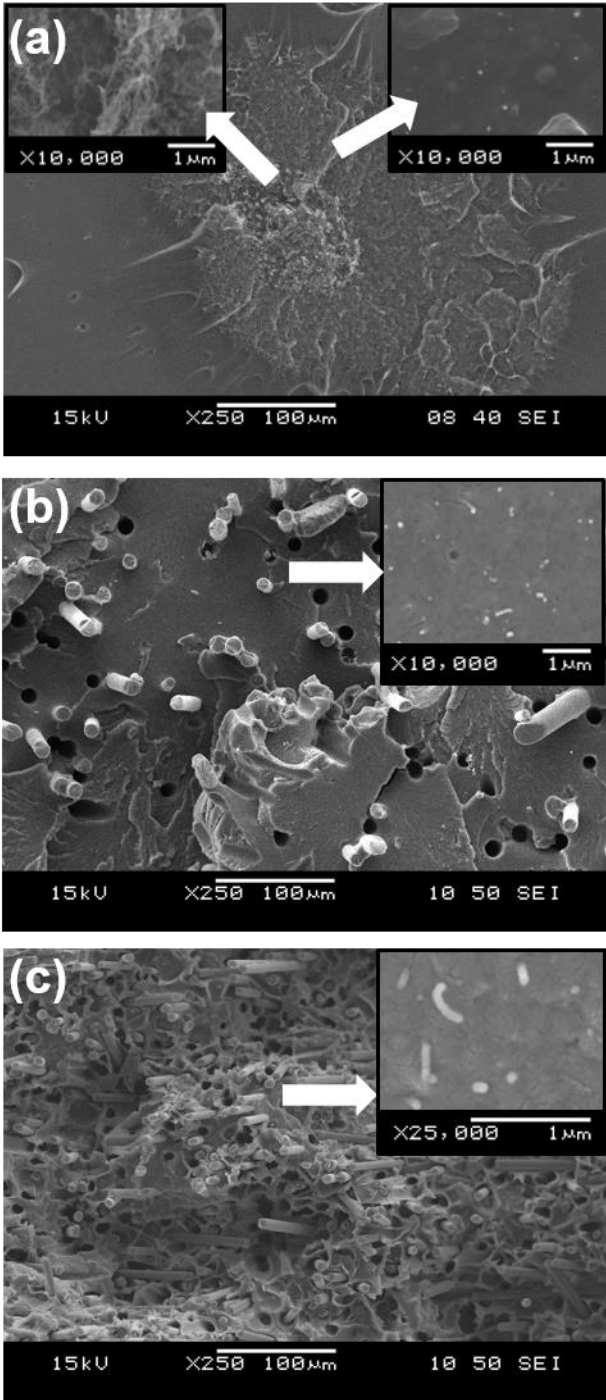
Fig. 1. *SEM micrographs of fracture surfaces: (a) PA6 / 0.25CNT; (b) PA6 / 30BF / 0.25CNT; (c) PA6 / 30CF / 0.25CNT*

(a)

PA6

PA6 / 0.25CNT

PA6 / 0.25CNT

PA6 / 0.75CNT

PA6 / 1CNT

4

Heat flow/mW g^{-1}

EXO

Temperature/°C

(b)

PA6 / 30BF

PA6 / 30BF / 0.25CNT

PA6 / 30BF / 0.5CNT

PA6 / 30BF / 0.75CNT

PA6 / 30BF / 1CNT

2

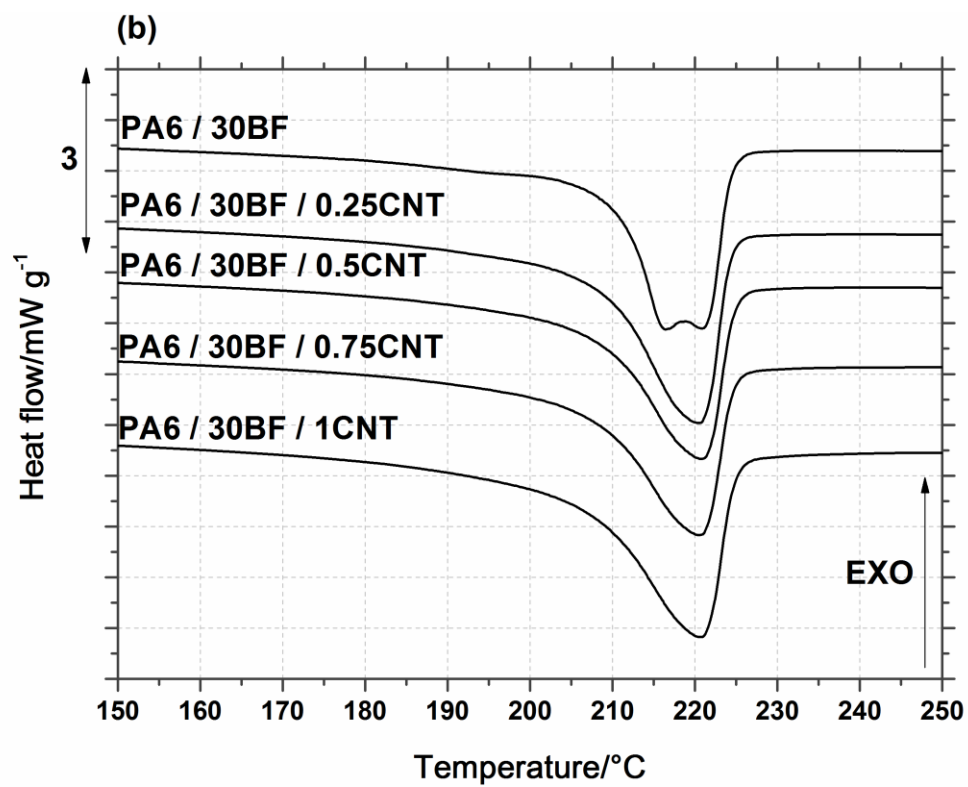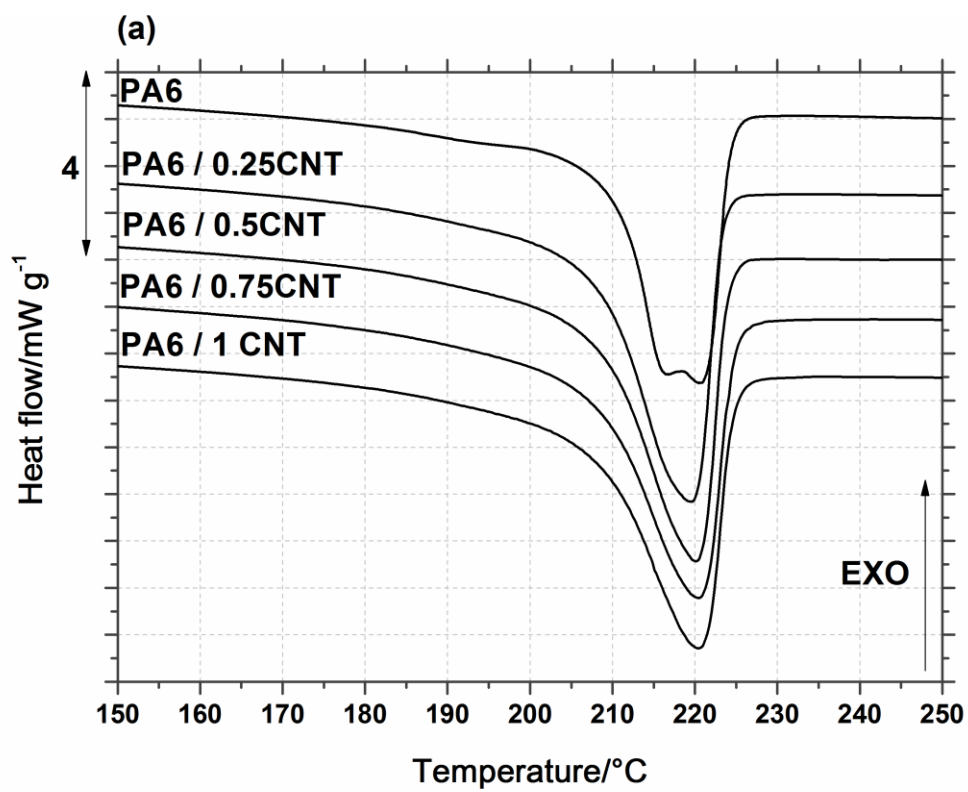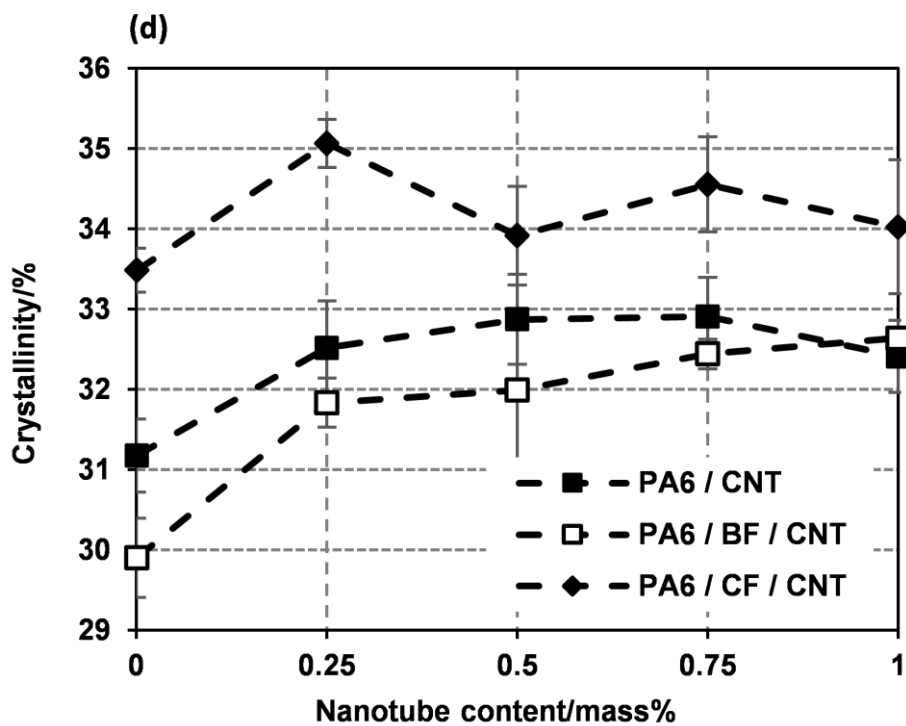Heat flow/mW g^{-1}

EXO

Temperature/°C

Fig. 2. *The heat flow of nanocomposites and hybrid composites (DSC) after the first heating: a) nanocomposites, b) basalt fiber reinforced composites and hybrid composites, c) carbon fiber reinforced composites and hybrid composites, d) crystallinity*

(a)

Heat flow/mW g^{-1}

5

EXO

PA6

PA6 / 0.25CNT

PA6 / 0.5CNT

PA6 / 0.75CNT

PA6 / 1 CNT

Temperature/°C

(b)

Heat flow/mW g^{-1}

5

EXO

PA6 / 30BF

PA6 / 30BF / 0.25CNT

PA6 / 30BF / 0.5CNT
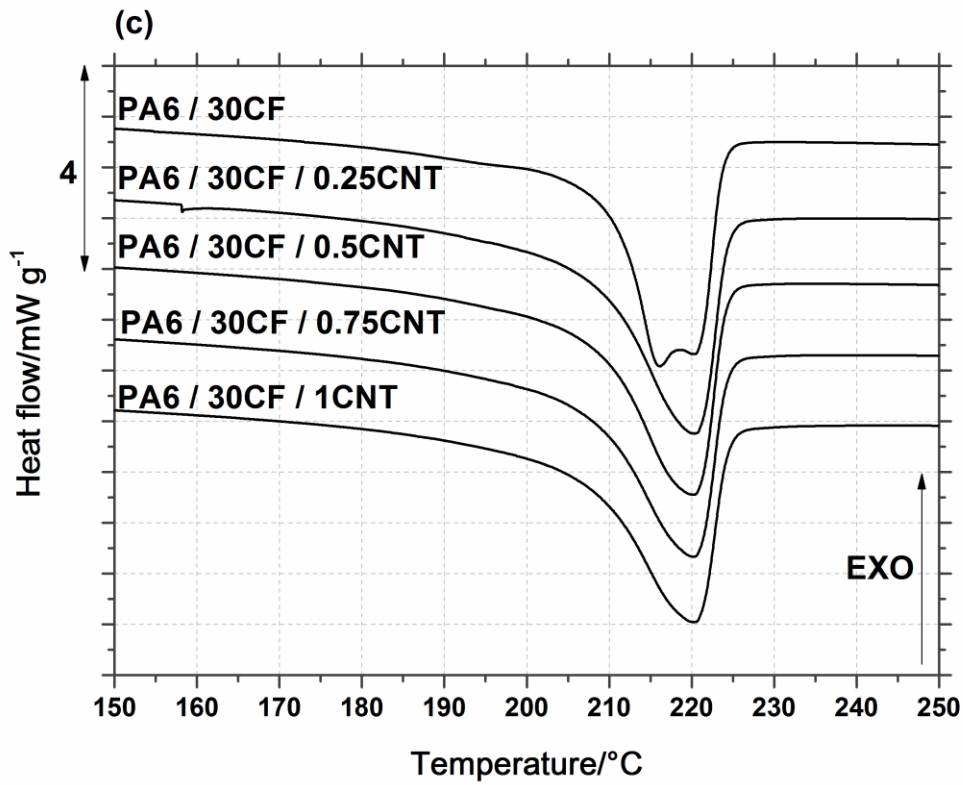
PA6 / 30BF / 0.75CNT

PA6 / 30BF / 1CNT

Temperature/°C

Fig. 3. *The heat flow of nanocomposites and hybrid composites (DSC) during cooling: a) nanocomposites, b) basalt fiber reinforced composites and hybrid composites, c) carbon fiber reinforced composites and hybrid composites*

(a)

PA6

PA6 / 0.25CNT

PA6 / 0.5CNT

PA6 / 0.75CNT

PA6 / 1 CNT

4

Heat flow/mW g^{-1}

EXO

Temperature/°C

(b)

PA6 / 30BF

PA6 / 30BF / 0.25CNT

PA6 / 30BF / 0.5CNT

PA6 / 30BF / 0.75CNT

PA6 / 30BF / 1CNT

3

Heat flow/mW g^{-1}

EXO

Temperature/°C

Fig. 4., *The heat flow of nanocomposites and hybrid composites (DSC) during the second heating: a) nanocomposites, b) basalt fiber reinforced composites and hybrid composites, c) carbon fiber reinforced composites and hybrid composites, d) crystallinity*
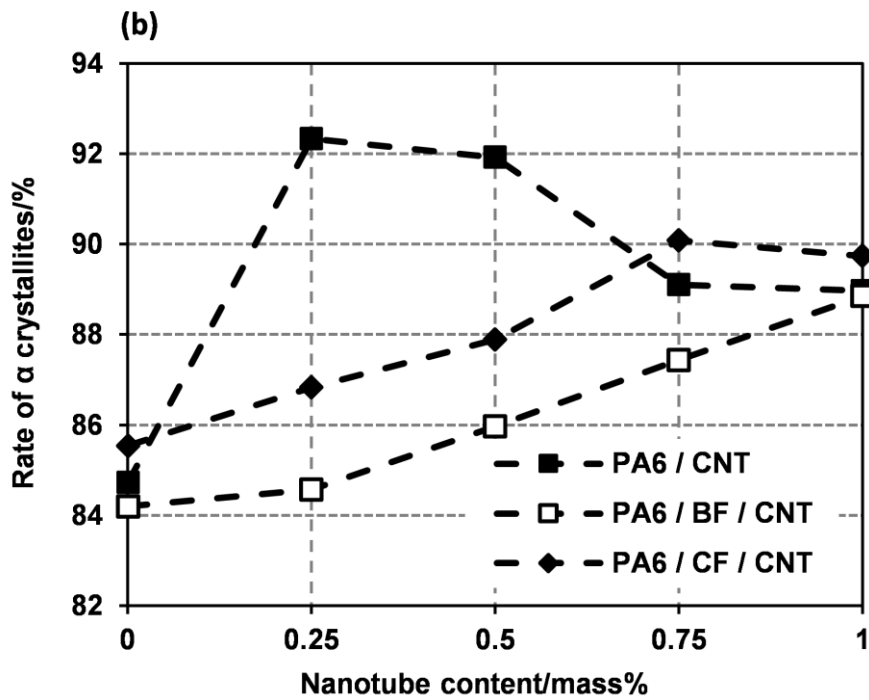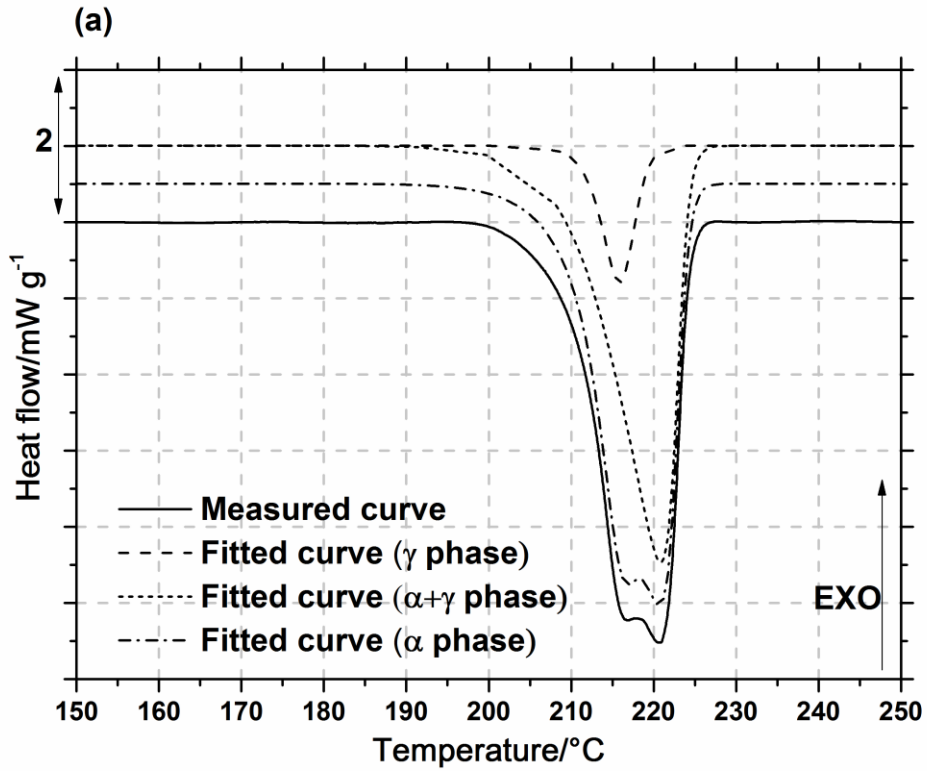
Fig. 5. *a) Melting curve and its decomposition with asymmetric double sigmoid curves b) The ratio of α crystals in composites as a percentage of total crystallinity*

Tables

Table 1. *Manufactured composites and their composition*

Sample code	PA6 /mass%	BF /mass%	CF /mass%	CNT /mass%
PA6	100	0	0	0
PA6 / 0.25CNT	99.75	0	0	0.25
PA6 / 0.5CNT	99.5	0	0	0.5
PA6 / 0.75CNT	99.25	0	0	0.75
PA6 / 1CNT	99	0	0	1
PA6 / 30BF	70	30	0	0
PA6 / 30BF / 0.25CNT	69.75	30	0	0.25
PA6 / 30BF / 0.5CNT	69.5	30	0	0.5
PA6 / 30BF / 0.75CNT	69.25	30	0	0.75
PA6 / 30BF / 1CNT	69	30	0	1
PA6 / 30CF	70	0	30	0
PA6 / 30CF / 0.25CNT	69.75	0	30	0.25
PA6 / 30CF / 0.5CNT	69.5	0	30	0.5
PA6 / 30CF / 0.75CNT	69.25	0	30	0.75
PA6 / 30CF / 1CNT	69	0	30	1

Table 2. *Tensile-mechanical properties of nano and hybrid composites [39]*

Sample code	Tensile strength /MPa	Tensile modulus /GPa	Elongation at break /%
PA6	52 ± 0.2	2.1 ± 0.1	45.1 ± 6.6
PA6 / 0.25CNT	50 ± 0.1	1.8 ± 0.1	48.3 ± 11.6
PA6 / 0.5CNT	50 ± 0.1	1.7 ± 0.2	47.4 ± 3.1
PA6 / 0.75CNT	50 ± 0.1	1.7 ± 0.1	46.1 ± 4.0
PA6 / 1CNT	50 ± 0.5	1.7 ± 0.2	38.5 ± 8.7
PA6 / 30BF	102 ± 1.3	6.2 ± 0.3	4.1 ± 1.0
PA6 / 30BF / 0.25CNT	111 ± 1.3	6.8 ± 0.1	3.4 ± 0.2
PA6 / 30BF / 0.5CNT	112 ± 1.1	7.2 ± 0.1	3.3 ± 0.1
PA6 / 30BF / 0.75CNT	111 ± 2.0	7.2 ± 0.3	3.3 ± 0.2
PA6 / 30BF / 1CNT	107 ± 1.5	7.0 ± 0.2	3.3 ± 0.2
PA6 / 30CF	179 ± 0.2	13.6 ± 0.2	2.6 ± 0.3
PA6 / 30CF / 0.25CNT	185 ± 1.6	13.8 ± 0.3	2.5 ± 0.2
PA6 / 30CF / 0.5CNT	198 ± 1.6	15.1 ± 0.4	2.4 ± 0.1
PA6 / 30CF / 0.75CNT	196 ± 1.5	15.2 ± 0.2	2.4 ± 0.1
PA6 / 30CF / 1CNT	194 ± 3.0	14.8 ± 0.2	2.4 ± 0.1

Table 3. *Crystalline melting temperatures and crystallization temperatures of the materials*

produced

Sample code	T_{m1}/°C	T_c/°C	T_{m2}/°C
PA6	222.0 ± 0.3	193.6 ± 0.1	220.4 ± 0.1
PA6 / 0.25CNT	221.4 ± 0.3	195.8 ± 0.2	219.4 ± 0.8
PA6 / 0.5CNT	221.0 ± 0.3	196.1 ± 0.4	219.7 ± 0.4
PA6 / 0.75CNT	221.2 ± 0.4	196.4 ± 0.1	219.9 ± 0.3
PA6 / 1CNT	221.1 ± 0.3	196.2 ± 0.1	220.2 ± 0.3
PA6 / 30BF	221.9 ± 1.4	193.3 ± 0.1	220.7 ± 0.3
PA6 / 30BF / 0.25CNT	221.5 ± 0.2	197.3 ± 0.2	220.4 ± 0.1
PA6 / 30BF / 0.5CNT	221.5 ± 0.5	196.9 ± 0.2	220.8 ± 0.1
PA6 / 30BF / 0.75CNT	221.3 ± 0.1	197.4 ± 0.1	220.5 ± 0.2
PA6 / 30BF / 1CNT	221.4 ± 0.4	197.3 ± 0.1	220.6 ± 0.3
PA6 / 30CF	221.6 ± 0.3	194.2 ± 0.5	220.3 ± 0.1
PA6 / 30CF / 0.25CNT	221.5 ± 0.1	197.3 ± 0.2	220.4 ± 0.1
PA6 / 30CF / 0.5CNT	221.4 ± 0.3	197.3 ± 0.1	220.2 ± 0.1
PA6 / 30CF / 0.75CNT	221.4 ± 0.1	197.5 ± 0.2	220.3 ± 0.1
PA6 / 30CF / 1CNT	221.1 ± 0.4	197.3 ± 0.5	220.3 ± 0.1